REPORT 1141

METHOD AND GRAPHS FOR THE EVALUATION OF AIR-INDUCTION SYSTEMS [1]

By George B. Brajnikoff

SUMMARY

Graphs have been developed for rapid evaluation of air-induction systems from considerations of their aerodynamic-performance parameters in combination with power-plant characteristics. The graphs cover the range of supersonic Mach numbers up to 3.0. Examples are presented for an air-induction system and engine combination at two Mach numbers and two altitudes in order to illustrate the method and application of the graphs. The examples show that jet-engine characteristics impose restrictions on the use of fixed inlets if the maximum net thrusts are to be realized at all flight conditions.

INTRODUCTION

In order to obtain a true indication of the worth of a given air-induction system as a component of a propulsive unit, it is necessary to employ an evaluation parameter that represents a summation of all the gains and penalties resulting from the use of that particular system. Such a parameter should consider not only the aerodynamics of the entire installation but also such factors as the weight, mechanical complexity, purpose of the aircraft, and many others. Obviously, such a universal parameter is difficult to derive and even more difficult to apply. For this reason, it is convenient to make a partial evaluation based on the aerodynamic considerations before attempting a general evaluation. In such a case, the net thrust or the net thermal efficiency can be used as figures of merit because they provide a measure of the aerodynamic and thermodynamic qualities of the installation. The net thrust represents the force remaining after subtraction of the drag chargeable to the propulsive system from the thrust that it develops. The net thermal efficiency may be obtained from the net thrust, the flight velocity, and the rate of fuel consumption.

The maximum net thrust and thermal efficiency attainable with a jet-engine installation depend greatly on the performance of the air-induction system employed. The characteristics of air-induction systems are usually presented in terms of total-pressure recovery, external drag coefficient, and mass-flow ratio. Unless all three of these parameters for one system excel those for another at supersonic speeds, it is difficult to choose the better system because of the interdependence of the engine and induction-system parameters. Because of this interdependence, it is necessary to combine the induction system and power-plant characteristics so as to obtain a single figure of merit for the complete installation. By comparing the figures of merit, it is possible to establish the relative aerodynamic worth of each of the air-induction systems considered when they are used with a given engine.

The effects of changes in various parameters on the overall performance of propulsive systems have been evaluated in the past (see refs. 1, 2, and 3); however, the scope of each of these investigations was limited because the magnitude of changes due to variations in parameters were determined for specific engines or specific installations. Therefore, the results have quantitative significance for the assumed installations only and cannot be applied directly to propulsive systems having component characteristics different from those used in the analyses.

The purpose of this report is to present a method of evaluation of various air-induction systems when combined with arbitrary jet engines, and to present graphs that were developed to permit rapid determination of the thrust coefficients of a wide variety of jet-propulsion systems (ram jets, turbojets with afterburning, ducted fans, etc.). The evaluation is based on considerations of the air-handling qualities of the induction systems and the component characteristics of engines. The method allows selection of the aerodynamically optimum combination of an induction system and engine for a particular set of flight conditions. Thus, it provides the initial solution in the more general problem that considers the relative merit of systems for a range of flight conditions.

NOTATION

A	cross-sectional area at any point of stream tube containing the air flowing through the propulsive system, sq ft
a	speed of sound, ft/sec
C_{D_p}	external drag coefficient of propulsive system based on maximum frontal area of installation, $\frac{D_p}{q_0 S^*}$, dimensionless
C_{D_p}'	external drag coefficient of propulsive system based on free-stream cross-sectional area of stream tube entering the inlet, $\frac{D_p}{q_0 A_0}$, dimensionless
C_{F_i}	internal thrust coefficient based on maximum frontal area of installation, $\frac{F_i}{q_0 S^*}$, dimensionless
C_{F_i}'	internal thrust coefficient based on the free-stream cross-sectional area of stream tube entering the inlet, $\frac{F_i}{q_0 A_0}$, dimensionless

[1] Supersedes NACA TN 2697, "Method and Graphs for the Evaluation of Air-Induction Systems," by George B. Brajnikoff, 1952.

C_{F_n}' net thrust coefficient based on the free-stream cross-sectional area of stream tube entering the inlet, $C_{F_t}'-C_{D_p}'$, dimensionless

C_{F_n} net thrust coefficient based on maximum frontal area of engine, dimensionless

D_p drag force chargeable to propulsive system if the engine thrust is defined as the total momentum at the exit station less that of the incoming flow in the free stream, $D_{(B+p)}-D_B+D_M$, lb

D_B pressure and friction drag forces acting on the basic body shape (fuselage) without an air inlet, lb

D_M total momentum of the incoming mass of air at the entrance station less the total momentum of the same mass of air in the free stream $[(p_1A_1+m_1V_1)-(p_0A_0+m_1V_0)]$, lb

$D_{(B+p)}$ pressure and friction drag forces acting on the external surface of the combined basic body and the propulsive system, lb

F_n net thrust force, F_t-D_p, lb

F_t internal thrust force (rate of momentum change of internal flow between free-stream and the tail-pipe exit where static pressure is assumed equal to the free-stream static pressure), lb

g acceleration due to gravity, ft/sec^2

h specific enthalpy, Btu/lb

J mechanical equivalent of heat, 778 ft-lb/Btu

L. H. V. lower heating value of fuel, Btu/lb

M Mach number, dimensionless

m mass-flow rate, slugs/sec

$\frac{m_1}{m_0}$ mass-flow ratio, $\frac{\rho_1 V_1 A_1}{\rho_0 V_0 A_1}$

n actual rotational speed of engine, rpm

$n_{corr.}$ corrected rotational speed, $n\sqrt{\frac{1.4\times519}{\gamma T_t}}$, (where γ and T_t correspond to stagnation conditions at the inlet of the unit under consideration), rpm

p static pressure, lb/sq ft

p_t total pressure, lb/sq ft

q dynamic pressure, lb/sq ft

S_P maximum frontal area of power plant, sq ft

S^* maximum frontal area of installation, sq ft

T static temperature, °R

T_t total temperature, °R

V speed, ft/sec

w weight-flow rate, lb/sec

γ ratio of specific heats

δ pressure correction factor, $\frac{p_t}{p_{sl}}$

η net thermal efficiency of propulsive system (net thrust times the flight speed divided by energy input rate)

$\eta_c\eta_t$ combined adiabatic efficiency of compressor and turbine

$\sqrt{\frac{1}{\theta}}$ temperature-correction factor, $\left(\frac{1.4\times519}{\gamma T_t}\right)^{\frac{1}{2}}$

ρ mass density, slugs/cu ft

SUBSCRIPTS

a air

B body

c compressor

D drag

F thrust

f fuel

i internal (within boundaries of stream tube entering the inlet)

M total momentum

M_a conditions corresponding to flight Mach number

n net

opt optimum conditions (conditions of best performance)

p propulsive system

P power plant

sl at standard sea-level static conditions

t stagnation conditions

0, 1, 2, 3....11 station, as shown in figure 1

SUPERSCRIPTS

$'$ based on free-stream area A_0

$*$ reference (such as frontal area, used in drag coefficient)

METHOD

The method of evaluation consists of determining the maximum net thrust coefficient based on the frontal area of the engine at various conditions of flight. The present report considers primarily the net thrust coefficient because the net thermal efficiency depends directly on the net thrust coefficient (see eq. (A8) of Appendix A); the evaluation at a given flight condition leads to the same conclusions, regardless of which of the two parameters is used. The net thermal efficiency is useful in evaluating complete flight plans when range and endurance must be considered.

In order to evaluate an induction system, the following information must be available:

1. The induction-system characteristics p_{t_3}/p_{t_0}, m_1/m_0, and C_{D_p} (which represents the total drag chargeable to the propulsive system) for various Mach numbers and ratios of inlet area to frontal area of the installation

2. The engine characteristics, such as the exhaust-to-inlet pressure and temperature ratios and the air-handling capacity (volume of air consumed per second)[2]

With this information, an inlet size can be selected for the propulsion system such that it operates at any desired mass-flow ratio and provides a constant volume of air as required by the engine. The inlet size and the mass-flow ratio in turn determine the external drag of the system.

[2] The ram-jet and turbojet engines operate essentially with constant-volume flow since the velocity past the flame holder and at the compressor intake must remain constant at the maximum allowable values. This condition is required in order to obtain the maximum thrust with an engine of a given frontal area.

By the use of the induction-system and engine-performance data corresponding to the operating condition, it is possible to calculate the net thrust coefficient.

In general, the method entails the following steps:

1. The thrust coefficient C_{F_t}', based on the free-stream area A_0 of the air required by the engine, is calculated for the given engine as a function of total-pressure recovery for the flight Mach number and altitude. This computation is performed using the induction-system characteristics (p_{t_3}/p_{t_0} as a function of m_1/m_0), the graphs presented in this report, and equation (A3) of Appendix A.

2. The drag coefficient attributable to the propulsive system at various mass-flow ratios, C_{D_p}, is transformed to C_{D_p}' by multiplying C_{D_p} by the ratio S^*/A_0. (See eq. (A4) of Appendix A.)

3. The net thrust coefficient C_{F_n}' (based on A_0) at various mass-flow ratios is obtained by subtracting the drag coefficient C_{D_p}' (step 2) from the thrust coefficient C_{F_t}' (step 1). (See Appendix A, eq. (A6).)

4. The net thrust coefficient C_{F_n} based on the frontal area of the engine is obtained by transforming C_{F_n}' (step 3) by means of equation (A7) of Appendix A.

After these calculations are performed for the range of operational mass-flow ratios, the maximum net thrust coefficient attainable with the given induction-system and engine combination is found from the plot of C_{F_n} as a function of m_1/m_0.

DETERMINATION OF THE MAXIMUM NET THRUST COEFFICIENT

Many air-induction systems produce highest total-pressure recoveries at mass-flow ratios less than the maximum attainable at a given supersonic Mach number. As the mass-flow ratio is reduced from its maximum value until the maximum total-pressure recovery is attained, the thrust coefficient C_{F_t}' increases due to rising recovery and so does the drag coefficient C_{D_p}' due to increasing additive drag (see ref. 4). Thus, in this range of mass-flow ratio, the total-pressure recovery and drag have opposite effects on the net thrust coefficient C_{F_n}'. To attain the maximum net thrust coefficient it is necessary, therefore, to provide the air required by the engine at an optimum mass-flow ratio that provides the best compromise between thrust and drag.

Determination of internal thrust coefficient, C_{F_i}'.—When calculations of the net thrust coefficient are made in order to find the optimum mass-flow ratio, it is convenient to consider the flow field existing about a propulsive system to be divided in two parts, internal and external, the boundary being that of the stream tube surrounding the air which enters the system. The flows within these two regions may be analyzed separately, and the results can be combined to obtain a figure of merit for the complete system. It is shown in Appendix A (eq. (A3)) that when the thrust due to internal flow is expressed in coefficient form (C_{F_t}') based on the free-stream area of the stream tube entering the induction system (A_0), the significance of the quantity of air required by the engine disappears. Then, the magnitude of C_{F_t}' depends only on the ratio of the exhaust and flight velocities. (The contribution of the mass of fuel burned, w_f/w_a, to the thrust, C_{F_t}', is usually on the order of only 5 percent at rated conditions and, for purposes of induction system comparison, may be neglected.) This fact makes it possible to isolate the effects of the total-pressure recovery on the thermodynamic cycle which determines the magnitude of the internal thrust coefficient C_{F_t}' attainable with given engine characteristics at a fixed Mach number and altitude. To reduce computational effort and to make the determination of the internal thrust coefficient universal, graphs based on the thermodynamic cycles of jet engines have been developed.

The processes undergone by the internal air flow from one station of a propulsion system to another have been represented graphically in figures 2 to 4 using the tables and methods of reference 5. (See example 16 of ref. 5 for illustration of the method of solution for various states of the gas.) The subscript numerals designate the stations shown in figure 1. The assumptions used are independent of any actual installation. They are as follows:

1. For a turbojet engine, the specific enthalpy change through the turbine is equal to the specific enthalpy rise in the compressor (calculated as if the compression were isentropic) divided by the product of the adiabatic efficiencies (the combined efficiency) of the two units.

2. The air-fuel ratios are those necessary to maintain the assigned combustion temperature by complete combustion of a fuel with the lower heating value (L. H. V.) equal to 19,000 Btu per pound.

3. The flow in the exhaust nozzle is isentropic; it has the properties of air at the exhaust temperatures and leaves the tail pipe at free-stream static pressure at all flight conditions. (This assumption requires an adjustable exhaust nozzle with variable throat and exit areas A_{10} and A_{11}.)

Flight and exhaust velocities can be determined from figure 2 for ram jets and also for turbojets if the engine performance is available in the generalized form (p_{t_9}/p_{t_3} and T_{t_9}/T_{t_3}) suggested in reference 6. If not, figures 3 to 5 must be used to find the effects of engine operation on the fluid conditions at the engine outlet or at the entrance of the exhaust nozzle. Quadrant I of figure 2 presents the variation of the free-stream Mach number with the speed of flight at various altitudes. Quadrant II yields the ratio of recovered total pressure to free-stream static pressure (p_{t_3}/p_0) as a function of total-pressure recovery (p_{t_3}/p_{t_0}) of the air-induction system. Quadrant III shows the highest exhaust Mach number obtainable with the available pressure ratio (p_{t_9}/p_0), which includes mechanical compression due to the power plant, as a function of the total temperature of the exhaust. The last quadrant provides the exhaust velocity corresponding to the exhaust Mach number and the total temperature T_{t_9} when $p_{11}=p_0$. A correction for the exhaust-nozzle losses can be applied to the exhaust velocity, which was calculated on the assumption of isentropic flow, if the actual-to-theoretical jet-speed ratio is known. (See ref. 4.)

The temperature graph, from which the total temperature at various stations throughout the propulsive system can be determined, is shown in figure 3. The effects of altitude, flight Mach number, mechanical compression, and burning of the fuel are included in this figure. Quadrant IV can be used to find the temperatures or the amounts of fuel consumed in afterburning as well as in the main combustion chambers. The effects of incomplete combustion or of a different fuel heating value on fuel consumption can be taken into account by direct ratios of combustion efficiencies or of the heating values. The temperature graph is used in conjunction with the compressor-turbine graph shown in figure 4 from which the turbine expansion ratio necessary to drive the compressor can be determined. This figure also provides the resulting total temperature at the turbine outlet (T_{t_6}) for a given inlet temperature.

Figure 5 presents the variation of the temperature correction factor with temperature at the compressor or turbine inlet. This figure is used to calculate the engine operational conditions from the performance parameters corrected to standard sea-level conditions. The effect of temperature on the ratio of specific heats for air has been included in the temperature correction factor for the compressor because the stagnation temperature of the free stream varies sufficiently to cause error if it were neglected.

The graphs described above allow determination of the velocities and air-fuel rates that must be known in order to calculate the internal thrust coefficient C_{F_i}'. The coefficient C_{F_i}' is computed by substituting these quantities in equation (A3) of Appendix A.

Determination of the external drag coefficient C_{D_p}.—The total drag chargeable to a propulsive unit consists of drag attributable to the induction system, to the modification of the airframe necessary to house the engine, and to the interference of the pressure field of the propulsive system with other components of the aircraft. The magnitude of drag chargeable to the induction system depends on the amount of diffusion ahead of the inlet, which is a function of mass-flow ratio (see ref. 7), and on the geometric proportions of the induction system which may be described, in general, by the length of the induction system and the ratio of inlet area to the frontal area of the installation (A_1/S^*). The inlet area necessary to provide the air required by the engine depends on the inlet mass-flow ratio; if the optimum mass-flow ratio is unknown, the value of the ratio A_1/S^* necessary for optimum operation is also unknown. Thus, when the optimum mass-flow ratio is being calculated, it is necessary to compute the variation of the net thrust coefficient C_{F_n} with mass-flow ratio for several values of A_1/S^* which are between the value for the inlet operating at the maximum mass-flow ratio and that required at the mass-flow ratio for maximum total-pressure recovery.

In practice, induction-system characteristics are usually obtained from tests with models having a fixed A_1/S^* ratio. If data for various ratios are unavailable, it is necessary to estimate the effects of A_1/S^* ratio on the total-pressure recovery and drag. The total-pressure recovery usually is not affected appreciably by small changes in the inlet size. The changes in drag, however, must be taken into consideration at a given mass-flow ratio, the additive drag varies directly with the inlet area, while the surface pressure drag, which is roughly proportional to the square of the angle of inclination of the external surface of the induction system with respect to the flow direction decreases slightly as the inlet area is increased.

DETERMINATION OF INLET SIZE FOR OPTIMUM OPERATION

To develop maximum thrust at a given flight condition with an engine operating with a fixed volumetric capacity, it is necessary to match the engine and the induction system so that the latter operates at the optimum mass-flow ratio. This condition is attained when the induction-system inlet area (A_1) is such that the cross-sectional area of the free-stream tube entering the inlet (A_0) is equal to that required by the engine. For a fixed volumetric capacity, the area A_0 required by the engine varies directly with the total-pressure recovery at the exit of the induction system. This area (A_0) can be found using relations given in Appendix B (see eqs. (B1) and (B8)) and the engine characteristics. The inlet area (A_1) can be found from the equation defining the mass-flow ratio, that is, $m_1/m_0=A_0/A_1$.

The engine air requirements change with Mach number and altitude, and the optimum mass-flow ratio usually changes with Mach number. Thus, it is unlikely that any one propulsive system will develop the maximum net thrust at all flight conditions unless the inlet area is adjustable. If the engine air requirements are adjusted to the characteristics of the induction system having a constant inlet area by means of engine-speed control, the propulsive system will not develop the attainable maximum net thrust at off-design flight conditions.[3] Appendix C presents the relations between the mass-flow ratio, the total-pressure recovery, and the engine air requirements at various engine speeds; these relations provide the information necessary for computation of engine performance at part-throttle operation.

ILLUSTRATIVE EXAMPLES

APPLICATION OF GRAPHS

The use of the graphs can be demonstrated best by illustrative examples. For this purpose a ram jet and a turbojet with and without afterburning have been selected. When the charts are used for determining the internal thrust coefficients of actual installations, the actual induction system and engine characteristics are used; in the present report, these characteristics have been assumed. The computations were performed for various total-pressure recoveries (p_{t_3}/p_{t_0} from 1.0 to 0.4) and Mach numbers (M_0 from 1.0 to 3.0) in order to obtain data for the example induction-system calculations presented later in this report.

Ram jet.—The steps of solution, presented in tabular form, for a ram jet flying at a Mach number 2.0 in the isothermal

[3] Since the engine ordinarily runs at the maximum speed allowable for continuous operation (rated rpm), the speed control can only reduce the speed. Thus, the weight of air handled per second and the operating temperature decrease with the result that thrust decreases.

region of the atmosphere are as follows (the assumed values are indicated by asterisks):

Item	Source	Units	Quantity
V_0	Fig. 2, quadrant I	$\frac{ft}{sec}$	1940
$\frac{p_{t_3}}{p_{t_0}}$	Induction-system characteristics	None	*0.80
$\frac{p_{t_3}}{p_0}$	Fig. 2, quadrant II	None	6.25
$T_{t_{0-3}}$	Fig. 3, quadrants I and II	° R	708
T_{t_9}	Operating temperature	° R	*3000
$\left(\frac{w_a}{w_f}\right)_s$	Fig. 3, for T_{t_9} and $T_{t_{0-3}}$	$\frac{\text{lb air}}{\text{lb fuel}}$	29.6
$\frac{p_{t_9}}{p_0}$	$\left(\frac{p_{t_3}}{p_0}\right)\left(\frac{p_{t_9}}{p_{t_3}}\right)$	None	6.25
V_{11}	Fig. 2, quadrants III and IV for p_{t_9}/p_0 and T_{t_9}.	None	3913
C_{F_i}'	$2\left[\left(1+\frac{w_f}{w_a}\right)\frac{V_{11}}{V_0}-1\right]$	None	2.170

The loss of total pressure between stations 3 and 9 was neglected. However, such loss can be taken into account by reducing the value of p_{t_9}/p_{t_3} by the amount of loss.

Figure 6 shows the variation of the internal thrust coefficient C_{F_i}' with the total-pressure recovery and Mach number computed using the procedure outlined in the sample calculation. The temperature of combustion was assumed to be 3000° R throughout the range of Mach numbers. It must be remembered in the use of this figure that, since a fixed temperature was used, either the size of the inlet or the mass-flow ratio must reduce with decreasing total-pressure recovery or the critical area of the exhaust nozzle must be increased to compensate for the greater specific volume of the air handled.

Turbojet.—In order to find the variation of the internal thrust coefficient for the turbojet without and with afterburning, the generalized characteristics of the engine shown in figure 7 were used. Constant actual speed n of 12,500 rpm (rated speed at standard intake conditions) was assumed for the entire range of operation in both cases. The compressor characteristics were selected so that the pressure ratio at Mach number 1.4 would be 6.25. (The reasons for selecting this pressure ratio are discussed in Appendix D.) The effects of Reynolds number index (the ratio of Reynolds number to Mach number, see ref. 6) on the compressor characteristics have been neglected. The turbine characteristics necessary to satisfy the engine operational requirements were determined using figures 3, 4, and 5 upon assumption of the variation of the adiabatic efficiency η_t with corrected turbine speed for sea-level static conditions. The operational limits were fixed by the assumptions of: (1) the combustion temperature (2000° R) at rated engine speed; (2) the equality of actual rotational speeds of compressor and turbine; and (3) the equality of compressor and turbine pressure ratios at the idling speed.

The internal thrust coefficients for the turbojet with afterburning were computed on the assumption that the total fuel consumption (engine plus afterburner) per pound of air is equal to that of the ram jet at the same Mach number. The steps of solution for the turbojet without and with afterburning are given in chronological order in table I which contains the computations for flight at Mach number 2.0 in the isothermal region of the atmosphere.

As in the case of the ram jet, the losses of total pressure due to combustion and friction $\left(\frac{p_{t_5}}{p_{t_4}}, \frac{p_{t_7}}{p_{t_6}}, \frac{p_{t_8}}{p_{t_7}}, \text{and } \frac{p_{t_9}}{p_{t_8}}\right)$ were neglected. Such losses, however, can be readily accounted for when p_{t_9}/p_0 is computed.

The variation of the internal-thrust coefficient C_{F_i}' with total-pressure recovery computed for a range of Mach numbers is shown in figure 8. The variations of the internal thrust coefficients with Mach number and total-pressure recovery were calculated for the engine characteristics pertaining to a fixed actual engine speed. Thus, as the total-pressure recovery decreases at a given Mach number and altitude, the size of the air inlet or the mass-flow ratio must be reduced for a fixed-size engine.

CALCULATION OF OPTIMUM MASS-FLOW RATIO AND INLET AREA

To illustrate the calculation of the maximum net thrust coefficient and of the required inlet area, the assumed characteristics of an air-induction system will be combined with the assumed engine characteristics shown in figure 7. In addition, the flight conditions of the example calculations will be selected so as to demonstrate the effects of Mach number and altitude on the maximum net thrust coefficient, the optimum mass-flow ratio, and the inlet area necessary for optimum performance.

Example 1.—Flight is in the isothermal region of the atmosphere at Mach number 2.5. The engine operates at the rated actual speed and uses afterburning to the extent that the total fuel consumption is equal to that of a ram jet having a 3000° R combustion temperature $T_{t_{8-9}}$. (See figs. 1 and 6.)

Example 2.—Flight is in the isothermal region of the atmosphere at Mach number 1.2. The engine operates at the rated actual speed and uses no afterburning.

Example 3.—Flight is at sea level at Mach number 1.2. The engine operates at the rated actual speed and uses no afterburning.

To simplify presentation, the effects of the ratio of inlet area to the maximum frontal area of the installation (A_1/S^*) on the drag coefficient and total-pressure recovery will be neglected; that is, the characteristics for a fixed (A_1/S^*) ratio will be used to find the optimum mass-flow ratio. The engine frontal area S_P will be assumed equal to 70 percent of S^*, and $A_1/S^*=0.20$ will be used in all examples; it will also be assumed that the engine operates at a constant speed (12,500 rpm) at all times, and that its size is such that it requires $A_0=1$ square foot when $p_{t_3}/p_{t_0}=1.0$ and $M_0=1.0$ at sea level, that is $(w_{a_{sl}})=54.6$ lb/sec.

The assumed characteristics of the induction system to be evaluated are shown in figures 9 and 10. This system, designed for $M_0=2.5$, uses one oblique shock wave ahead of the entrance and a normal shock wave just inside the inlet

at the maximum mass-flow ratio. The A_1/S^* ratio is typical of induction systems of the side-scoop type. At $M_0=1.2$, the maximum mass-flow ratio is less than at $M_0=2.5$ because the normal shock wave is well ahead of the entrance and a considerable portion of flow is deflected past the inlet. For the same reason, the minimum external drag coefficient C_{D_p} is higher as a result of a greater additive drag coefficient (see ref. 7). The total-pressure recovery is higher at $M_0=1.2$ because the normal shock wave occurs at a lower Mach number.

In all cases the solution follows the outline given in the section entitled "Method" of this report.

Step 1: The variation of the internal thrust coefficient C_{F_i}' with p_{t_3}/p_{t_0} at flight Mach number and altitude is calculated. Figure 11 shows the internal thrust coefficient C_{F_i}' for example 1 obtained from the cross plot of data of figure 8 for $M_0=2.5$.

Step 2: The external drag coefficients shown in figure 9, when converted to A_0 using equation (A4) of Appendix A and $A_1/S^*=0.20$, assume the values shown in figure 11.

Step 3: The net thrust coefficient C_{F_n}' is obtained by subtracting C_{D_p}' from C_{F_i}' of figure 11.

Step 4: The net thrust coefficient C_{F_n}, obtained using the relation

$$C_{F_n}=C_{F_n}'\left(\frac{A_1}{S_P}\right)\left(\frac{m_1}{m_0}\right)=C_{F_n}'\left(\frac{A_1}{S^*}\right)\left(\frac{m_1}{m_0}\right)\left(\frac{S^*}{S_P}\right)$$

$$=0.286\,C_{F_n}'\left(\frac{m_1}{m_0}\right)$$

and the values found in step 3, are shown in figure 12 for example 1.

Similar calculations for examples 2 and 3 yield the results shown in figure 13. In the case of example 3, curves similar to those of figure 8 for sea-level flight must be used.

The free-stream-tube area necessary to supply the air required by the turbojet engine of the illustrative examples is shown in figure 14 for various Mach numbers and total-pressure recoveries at two altitudes. The curves shown were obtained using equation (B8) of Appendix B. The inlet areas required at each of the three flight conditions to produce maximum net thrust coefficients C_{F_n} were obtained by dividing the free-stream areas A_0, required by the engine when the total-pressure recoveries are equal to those at $\left(\frac{m_1}{m_0}\right)_{opt}$, by the respective $\left(\frac{m_1}{m_0}\right)_{opt}$.

The results of the calculations are summarized in the following table:

Example	$\left(\frac{m_1}{m_0}\right)_{opt}$	Maximum C_{F_n}	Optimum inlet area $(A_1)_{opt}$ sq ft
1	1.65	0.750	0.794
2	.94	.450	1.075
3	.94	.149	.915

These results indicate that the inlet area required for optimum performance must change with altitude at a fixed Mach number, as well as with Mach number at a fixed altitude. Although the results depend entirely on the variation of the induction system and engine characteristics with Mach number and altitude, it is unlikely that any one propulsive system will develop the attainable maximum net thrust throughout the range of Mach numbers and altitudes unless some means of varying the inlet area are employed.

AMES AERONAUTICAL LABORATORY,
NATIONAL ADVISORY COMMITTEE FOR AERONAUTICS,
MOFFETT FIELD, CALIF., *February 19, 1952.*

APPENDIX A

RELATIONS DESCRIBING NET THRUST COEFFICIENT AND NET THERMAL EFFICIENCY

The internal thrust force and the internal thrust coefficient are given by the following relations when the exhaust pressure is equal to free-stream static pressure:

$$F_i=\frac{w_a}{g}\left[\left(1+\frac{w_f}{w_a}\right)V_{11}-V_0\right]$$

$$=\rho_0 A_0 V_0^2\left[\left(1+\frac{w_f}{w_a}\right)\frac{V_{11}}{V_0}-1\right]=2q_0A_0\left[\left(1+\frac{w_f}{w_a}\right)\frac{V_{11}}{V_0}-1\right] \tag{A1}$$

$$C_{F_i}=\frac{F_i}{q_0S^*}=2\frac{A_0}{S^*}\left[\left(1+\frac{w_f}{w_a}\right)\frac{V_{11}}{V_0}-1\right] \tag{A2}$$

where w_f/w_a represents the total amount of fuel consumed per pound of air handled. When based on the free-stream area of the stream tube entering the duct, the internal thrust coefficient is given by

$$C_{F_i}'=C_{F_i}\frac{S^*}{A_0}=2\left[\left(1+\frac{w_f}{w_a}\right)\frac{V_{11}}{V_0}-1\right] \tag{A3}$$

Similarly,

$$C_{D_p}'=C_{D_p}\frac{S^*}{A_0}=C_{D_p}\frac{S^*}{A_1\dfrac{m_1}{m_0}} \tag{A4}$$

where $\dfrac{m_1}{m_0}=\dfrac{\rho_1V_1A_1}{\rho_0V_0A_1}$ by definition. By continuity, $\rho_1V_1A_1=\rho_0V_0A_0$, and thus $\dfrac{m_1}{m_0}=\dfrac{\rho_0V_0A_0}{\rho_0V_0A_1}=\dfrac{A_0}{A_1}$.

The net thrust coefficient based on A_0 is given by

$$C_{F_n}'=C_{F_i}'-C_{D_p}' \tag{A5}$$

thus,

$$C_{F_n}'=2\left[\left(1+\frac{w_f}{w_a}\right)\frac{V_{11}}{V_0}-1\right]-C_{D_p}\frac{S^*}{A_1\dfrac{m_1}{m_0}} \tag{A6}$$

The net thrust coefficient based on the engine frontal area is related to C_{F_n}' by the following relation:

$$C_{F_n}=C_{F_n}'\left(\frac{A_1}{S_P}\right)\left(\frac{m_1}{m_0}\right)=C_{F_n}'\left(\frac{A_1}{S^*}\right)\left(\frac{S^*}{S_P}\right)\left(\frac{m_1}{m_0}\right) \tag{A7}$$

The net thermal efficiency of a propulsive system is given as

$$\eta=\frac{F_nV_0}{[(\text{L. H. V.})\,w_f]J}$$

where

$$F_n=C_{F_n}'\frac{1}{2}\rho_0V_0^2A_0=\frac{1}{2}C_{F_n}'(\rho_0V_0A_0)V_0=\frac{1}{2}C_{F_n}'\frac{w_a}{g}V_0$$

thus

$$\eta=\frac{1}{2}\frac{C_{F_n}'V_0^2}{(\text{L. H. V.})\,gJ}\frac{w_a}{w_f} \tag{A8}$$

where w_a/w_f is the weight ratio of air to fuel for the complete installation.

If fuel is added at stations A and B and the local w_a/w_f ratios are known, it can be shown that

$$\left(\frac{w_a}{w_f}\right)_{total}=\frac{\left[\left(\dfrac{w_a}{w_f}\right)_A+1\right]\left[\left(\dfrac{w_a}{w_f}\right)_B+1\right]}{\left(\dfrac{w_a}{w_f}\right)_A+\left(\dfrac{w_a}{w_f}\right)_B+2}-1$$

since for one pound of mixture (see ref. 5)

$$\left(\frac{w_f}{w_a+w_f}\right)_{total}=\left(\frac{w_f}{w_a+w_f}\right)_A+\left(\frac{w_f}{w_a+w_f}\right)_B$$

Similarly, solving for the air-to-fuel ratio necessary to make up a total ratio,

$$\left(\frac{w_a}{w_f}\right)_B=\frac{\left[\left(\dfrac{w_a}{w_f}\right)_A+1\right]\left[\left(\dfrac{w_a}{w_f}\right)_{total}+1\right]}{\left(\dfrac{w_a}{w_f}\right)_A-\left(\dfrac{w_a}{w_f}\right)_{total}}-1 \tag{A9}$$

APPENDIX B

RELATION BETWEEN ENGINE REQUIREMENTS AND THE OPTIMUM INLET AREAS AT VARIOUS FLIGHT CONDITIONS

The corrected air flow given by the relation

$$(w_a)_{corr.\,c}=\left(w_a\frac{\sqrt{\theta_3}}{\delta_3}\right)_{M_a}$$

can be plotted in the form of a ratio to the rated corrected value

$$(w_a)_{sl}=\left(w_a\frac{\sqrt{\theta_3}}{\delta_3}\right)_{sl}$$

Thus

$$\frac{(w_a)_{corr.\,c}}{(w_a)_{sl}}=\frac{\left(w_a\dfrac{\sqrt{\theta_3}}{\delta_3}\right)_{M_a}}{\left(w_a\dfrac{\sqrt{\theta_3}}{\delta_3}\right)_{sl}}$$

or

$$(w_a)_{M_a}=\left(w_a\frac{\sqrt{\theta_3}}{\delta_3}\right)_{sl}\frac{(w_a)_{corr.\,c}}{(w_a)_{sl}}\left(\frac{\delta_3}{\sqrt{\theta_3}}\right)_{M_a} \tag{B1}$$

where $(w_a)_{M_a}=g\rho_0V_0A_0$ is the actual weight rate of air flow through the engine at a given Mach number. For any two Mach numbers M_{a_1} and M_{a_2} the weight rates are thus related by the ratio

$$\frac{(w_a)_{M_{a_1}}}{(w_a)_{M_{a_2}}}=\frac{\left[\dfrac{(w_a)_{corr.\,c}}{(w_a)_{sl}}\left(\dfrac{\delta_3}{\sqrt{\theta_3}}\right)\right]_{M_{a_1}}}{\left[\dfrac{(w_a)_{corr.\,c}}{(w_a)_{sl}}\left(\dfrac{\delta_3}{\sqrt{\theta_3}}\right)\right]_{M_{a_2}}} \tag{B2}$$

for a given engine.

The weight flow in the free stream through an area equal to that of inlet passage is given by the relation $g\rho_0V_0A_1=g\rho_0M_0A_1a_0$ and the weight entering the inlet is given by

$$(w_a)_{M_a}=\left[(g\rho_0M_0A_1a_0)\frac{m_1}{m_0}\right]_{M_a} \tag{B3}$$

At any two Mach numbers M_{a_1} and M_{a_2}

$$\frac{(w_a)_{M_{a_1}}}{(w_a)_{M_{a_2}}}=\frac{\left(g\rho_0M_0A_1a_0\dfrac{m_1}{m_0}\right)_{M_{a_1}}}{\left(g\rho_0M_0A_1a_0\dfrac{m_1}{m_0}\right)_{M_{a_2}}} \tag{B4}$$

If the two static pressures and temperatures are equal (fixed standard altitude)

$$\frac{(w_a)_{M_{a_1}}}{(w_a)_{M_{a_2}}}=\frac{\left(A_1M_0\frac{m_1}{m_0}\right)_{M_{a_1}}}{\left(A_1M_0\frac{m_1}{m_0}\right)_{M_{a_2}}} \tag{B5}$$

The flow through the inlet must be equal to the flow through the engine for a matched condition. Thus,

$$\frac{\left(A_1M_0\frac{m_1}{m_0}\right)_{M_{a_1}}}{\left(A_1M_0\frac{m_1}{m_0}\right)_{M_{a_2}}}=\frac{\left[\frac{(w_a)_{corr.\,c}}{(w_a)_{sl}}\frac{\delta_3}{\sqrt{\theta_3}}\right]_{M_{a_1}}}{\left[\frac{(w_a)_{corr.\,c}}{(w_a)_{sl}}\frac{\delta_3}{\sqrt{\theta_3}}\right]_{M_{a_2}}}$$

since $\delta_3=\frac{p_{t_3}}{p_0}\frac{p_0}{p_{sl}}$ and $\frac{p_0}{p_{sl}}$=constant for a fixed altitude,

$$\frac{(A_1)_{M_{a_2}}}{(A_1)_{M_{a_1}}}=\frac{\left[M_0\left(\frac{m_1}{m_0}\right)_{opt}\right]_{M_{a_1}}\left[\frac{(w_a)_{corr.\,c}}{(w_a)_{sl}}\frac{p_{t_3}}{p_0}\sqrt{\frac{1}{\theta_3}}\right]_{M_{a_2}}}{\left[M_0\left(\frac{m_1}{m_0}\right)_{opt}\right]_{M_{a_2}}\left[\frac{(w_a)_{corr.\,c}}{(w_a)_{sl}}\frac{p_{t_3}}{p_0}\sqrt{\frac{1}{\theta_3}}\right]_{M_{a_1}}} \tag{B6}$$

or

$$\frac{(A_1)_{M_2}}{(A_1)_{M_1}}=\frac{\left[M_0\left(\frac{m_1}{m_0}\right)_{opt}\right]_{M_{a_1}}\left[\frac{(w_a)_{corr.\,c}}{(w_a)_{sl}}\frac{p_{t_3}}{p_{t_0}}\frac{p_{t_0}}{p_0}\sqrt{\frac{1}{\theta_3}}\right]_{M_{a_2}}}{\left[M_0\left(\frac{m_1}{m_0}\right)_{opt}\right]_{M_{a_2}}\left[\frac{(w_a)_{corr.\,c}}{(w_a)_{sl}}\frac{p_{t_3}}{p_{t_0}}\frac{p_{t_0}}{p_0}\sqrt{\frac{1}{\theta_0}}\right]_{M_{a_1}}}$$

The values of $\frac{(w_a)_{corr.\,c}}{(w_a)_{sl}}$ are given by the engine (compressor) characteristics for corrected compressor speed $n_{corr.\,c}$, which may be found using figures 3 and 5. The rest of the terms are determined from the inlet characteristics and flight conditions with the help of figures 2, 3, and 5.

For flight at different altitudes and Mach numbers it can be shown, similarly to equation (B6), that

$$\frac{(A_1)_{M_{a_2}}}{(A_1)_{M_{a_1}}}=\frac{\left[M_0\left(\frac{m_1}{m_0}\right)_{opt}\frac{p_0}{p_{t_0}}\right]_{M_{a_1}}\left[\frac{(w_a)_{corr.\,c}}{(w_a)_{sl}}\frac{p_{t_3}}{p_{t_0}}\frac{a_0}{a_{t_0}}\right]_{M_{a_2}}}{\left[M_0\left(\frac{m_1}{m_0}\right)_{opt}\frac{p_0}{p_{t_0}}\right]_{M_{a_2}}\left[\frac{(w_a)_{corr.\,c}}{(w_a)_{sl}}\frac{p_{t_3}}{p_{t_0}}\frac{a_0}{a_{t_0}}\right]_{M_{a_1}}} \tag{B7}$$

where $a_t=\sqrt{\gamma_3 gRT_{t_3}}$ is the speed of sound at stagnation conditions.

The free-stream area A_0 required by the engine at various flight conditions can be obtained using equation (B7) by letting $\left(\frac{m_1}{m_0}\right)_{opt}=1$, and $A_1=A_0$. Thus

$$\frac{(A_0)_{M_2}}{(A_0)_{M_1}}=\frac{\left(M_0\frac{p_0}{p_{t_0}}\right)_{M_{a_1}}\left[\frac{(w_a)_{corr.\,c}}{(w_a)_{sl}}\frac{p_{t_3}}{p_{t_0}}\frac{a_0}{a_{t_0}}\right]_{M_{a_2}}}{\left(M_0\frac{p_0}{p_{t_0}}\right)_{M_{a_2}}\left[\frac{(w_a)_{corr.\,c}}{(w_a)_{sl}}\frac{p_{t_3}}{p_{t_0}}\frac{a_0}{a_{t_0}}\right]_{M_{a_1}}} \tag{B8}$$

where $\frac{p_0}{p_{t_0}}=\frac{1}{p_{t_3}/p_0}$ when $\frac{p_{t_3}}{p_{t_0}}=1.0$. Quadrant II of figure 2 gives $\frac{p_{t_3}}{p_0}$ for M_0.

$$\frac{a_0}{a_t}=\frac{a_0}{a_{sl}}\frac{a_{sl}}{a_t}=\frac{a_0}{a_{sl}}\sqrt{\frac{1.4\times 519}{\gamma T_t}}=\frac{a_0}{a_{sl}}\sqrt{\frac{1}{\theta}}$$

where

$\frac{a_0}{a_{sl}}$ is the ratio of speed of sound at static temperature for flight altitude to that at standard sea-level conditions. This ratio can be found from quadrant I of figure 2.

$\sqrt{\frac{1}{\theta}}$ is given in figure 5 for $T_t\equiv T_{t_{0-3}}$ which can be found from quadrants I and II of figure 3.

APPENDIX C

RELATION BETWEEN INLET MASS-FLOW RATIO AND THE ENGINE AIR REQUIREMENTS AT A FIXED MACH NUMBER AND ALTITUDE

The mass-flow ratio, by definition, is given by

$$\frac{m_1}{m_0}=\frac{\rho_1 V_1 A_1}{\rho_1 V_0 A_1}$$

The mass of air flowing through the inlet is then

$$\rho_1 V_1 A_1=\frac{m_1}{m_0}\rho_0 V_0 A_1$$

The weights of air flowing through the inlet and the engine are equal and are given by

$$w_a=\frac{m_1}{m_0}g\rho_0 V_0 A_1=(w_a)_{corr.\,c}\left(\frac{\delta_3}{\sqrt{\theta_3}}\right)_{M_a}$$

and

$$\left(\frac{m_1}{m_0}\right)_{opt}g\rho_0 V_0 A_1=\left[(w_a)_{corr.\,c}\left(\frac{\delta_3}{\sqrt{\theta_3}}\right)_{M_a}\right]_{opt}$$

Thus, the ratio of mass flows at different m_1/m_0 is given by

$$\frac{\frac{m_1}{m_0}}{\left(\frac{m_1}{m_0}\right)_{opt}}=\frac{\left[(w_a)_{corr.\,c}\left(\frac{\delta_3}{\sqrt{\theta_3}}\right)_{M_a}\right](w_a)_{sl}}{\left[(w_a)_{corr.\,c}\left(\frac{\delta_3}{\sqrt{\theta_3}}\right)_{M_a}\right]_{opt}(w_a)_{sl}}$$

or

$$\frac{\frac{m_1}{m_0}}{\left(\frac{m_1}{m_0}\right)_{opt}}=\frac{\left[\frac{(w_a)_{corr.\,c}}{(w_a)_{sl}}\left(\frac{\delta_3}{\sqrt{\theta_3}}\right)_{M_a}\right]}{\left[\frac{(w_a)_{corr.\,c}}{(w_a)_{sl}}\left(\frac{\delta_3}{\sqrt{\theta_3}}\right)_{M_a}\right]_{opt}} \tag{C1}$$

Solving for $\frac{(w_a)_{corr.\,c}}{(w_a)_{sl}}$ and rearranging terms, one obtains

$$\left.\frac{(w_a)_{corr.\,c}}{(w_a)_{sl}}\right|_{\frac{m_1}{m_0}}=\left[\frac{(w_a)_{corr.\,c}}{(w_a)_{sl}}\right]_{opt}\frac{\frac{m_1}{m_0}}{\left(\frac{m_1}{m_0}\right)_{opt}}\frac{\left[\left(\frac{\delta_3}{\sqrt{\theta_3}}\right)_{M_a}\right]_{opt}}{\left(\frac{\delta_3}{\sqrt{\theta_3}}\right)_{M_a}} \tag{C2}$$

For a given Mach number and altitude the total temperature $T_{t_{0-3}}$ is constant, hence

$$[(\sqrt{\theta_3})_{M_a}]_{opt}=(\sqrt{\theta_3})_{M_a}$$

By definition,

$$\delta_3=p_{t_3}/p_{sl}$$

or

$$\delta_3=\frac{p_{t_3}p_{t_0}}{p_{t_0}p_{sl}}=\frac{p_{t_3}}{p_{t_0}}\frac{p_{t_0}}{p_0}\frac{p_0}{p_{sl}}$$

where $\frac{p_{t_0}}{p_{sl}}$=constant for a given M_0 and altitude. Thus,

$$\left.\frac{(w_a)_{corr.\,c}}{(w_a)_{sl}}\right|_{\frac{m_1}{m_0}} = \left[\frac{(w_a)_{corr.\,c}}{(w_a)_{sl}}\right]_{opt} \frac{\frac{m_1}{m_0}}{\left(\frac{m_1}{m_0}\right)_{opt}} \frac{\left(\frac{p_{t_3}}{p_{t_0}}\right)_{opt}}{\left(\frac{p_{t_3}}{p_{t_0}}\right)_{\frac{m_1}{m_0}}} \qquad \text{(C3)}$$

Using $\left.\frac{(w_a)_{corr.\,c}}{(w_a)_{sl}}\right|_{\frac{m_1}{m_0}}$, the compressor corrected speed $n_{corr.\,c}$ can be found from the engine characteristics. The actual engine speed n can be found, once $\sqrt{\theta_3}$ is known, since $n = n_{corr.\,c}\sqrt{\theta_3}$

APPENDIX D

SELECTION OF COMPRESSOR PRESSURE RATIO

The compressor pressure ratio p_{t_4}/p_{t_3}, as used in this report, has been selected using the maximum obtainable internal thrust coefficient as a criterion. Figures 2, 3, and 4 were used together with the equation for the internal thrust coefficient C_{F_4}, (Appendix A, eq. (A3)). The calculations were based on the following principles:

1. In order to segregate the effects of variation of engine parameters from the effects of altitude and pressure recovery, the conditions of the isothermal region of the atmosphere were used and isentropic recovery was assumed.

2. The combined efficiency of the compressor and turbine $\eta_c\eta_t$ was assumed to be 100 percent in all computations, and a combustion temperature of 2000° R was used.

3. The internal thrust coefficient C_{F_t}' was determined for assumed Mach numbers of flight. The exhaust nozzle was considered 100 percent efficient.

The results of these calculations are shown in figure 15 for the turbojet without afterburning. The points of maximum internal thrust coefficients have been joined by a curve which indicates the compressor pressure ratios necessary to obtain optimum operation. The data of figure 15 are idealized since the variation in compressor efficiency with temperature was not included ($\eta_c\eta_t$ was assumed to be 100 percent).

The optimum pressure ratios, however, are not affected appreciably by the combined efficiency; the thrust coefficients, on the contrary, are largely dependent on efficiency of every component of an installation. Pressure ratios of the compressor of figure 7 at various Mach numbers also are shown in figure 15. The value of $p_{t_4}/p_{t_3}=6.25$ at $M_0=1.4$ was selected as one that would produce approximately maximum internal thrust coefficient without afterburning at Mach numbers less than 2.0. Figure 16, which presents data similar to those of figure 15 but with afterburning, shows that the same engine using afterburning is capable of producing nearly maximum internal thrust coefficients in the range of Mach numbers between 2.0 and 3.0. Again, the amount of afterburning was controlled so that total fuel consumption would be equal to that of the ram jet of figure 6.

REFERENCES

1. Wood, George P.: Performance Possibilities of the Turbojet System as a Power Plant for Supersonic Airplanes. NACA RM L7HO5a, 1947.
2. Hanson, Frederick H., Jr., and Mossman, Emmet A.: Effect of Pressure Recovery on the Performance of a Jet-Propelled Airplane. NACA TN 1695, 1948.
3. Keirn, D. J., and Shoults, D. R.: Jet Propulsion and Its Application to High-Speed Aircraft. Jour. Aero. Sci., vol. 13, no. 8, Aug. 1946, pp. 411–424.
4. Luskin, H., and Klein, H.: High-Speed Aerodynamic Problems of Turbojet Installations. Douglas Aircraft Company Rept. SM–13830, Sept. 1, 1950.
5. Keenan, Joseph H., and Kaye, Joseph: Gas Tables. Thermodynamic Properties of Air, Products of Combustion and Component Gases. Compressible Flow Functions. John Wiley and Sons, Inc., N. Y., 1948.
6. Sanders, Newell D., and Behun, Michael: Generalization of Turbojet-Engine Performance in Terms of Pumping Characteristics. NACA TN 1927, 1949.
7. Wyatt, DeMarquis D.: Aerodynamic Forces Associated with Inlets of Turbojet Installations. Aeronautical Engineering Review Oct. 1951, p. 20.

TABLE I.—SAMPLE CALCULATIONS FOR A TURBOJET ENGINE WITH AND WITHOUT AFTERBURNING.

Item	Source	Units	Turbojet without afterburning	Turbojet with afterburning
V_0	Fig. 2, quadrant I	$\frac{ft}{sec}$	1940	1940
p_{t_3}/p_{t_0}	Induction-system characteristics	None	° 0.80	° 0.80
p_{t_3}/p_0	Fig. 2, quadrant II	None	6.25	6.25
$T_{t_{0-3}}$	Fig. 3, quadrants I and II	° R	708	708
$\sqrt{\frac{1}{\theta_3}}$	Fig. 5, for T_{t_3}	None	0.858	0.858
n	Actual engine speed	rpm	° 12,500	° 12,500
$n_{corr.\,c}$	$n\sqrt{\frac{1}{\theta_3}}$	rpm	° 10,720	° 10,720
η_c	Compressor characteristics for $n_{corr.\,c}$, fig. 7.	None	° 0.900	° 0.900
p_{t_4}/p_{t_3}	Compressor characteristics for $n_{corr.\,c}$, fig. 7.	None	° 4.56	° 4.56
T_{t_4}	Fig. 3 for p_{t_4}/p_{t_3} and $T_{t_{0-3}}$	° R	1060	1060
T_{t_5}	Engine characteristics for $n_{corr.\,c}$, fig. 7.	° R	° 2000	° 2000
$\sqrt{\frac{1}{\theta_5}}$	Fig. 5 for T_{t_5}	None	0.522	0.522
$n_{corr.\,t}$	$n\sqrt{\frac{1}{\theta_5}}$	rpm	6530	6530
η_t	Turbine characteristics for $n_{corr.\,t}$, fig. 7.	None	° 0.900	° 0.900
p_{t_5}/p_{t_6}	Fig. 4 for T_{t_3}, $\eta_c\eta_t$, and T_{t_5}	None	2.50	2.50
T_{t_6}	Fig. 4 for p_{t_5}/p_{t_6} and T_{t_5}	° R	1584	1584
$\left(\frac{w_a}{w_f}\right)_5$	Fig. 3 for T_{t_4} and T_{t_5}	$\frac{lb\ air}{lb\ fuel}$	77.06	77.06
$\left(\frac{w_a}{w_f}\right)$ total at station 8.	Assumed equal to that of ram jet operating at 3000° R.	$\frac{lb\ air}{lb\ fuel}$	-------	° 29.6
$\left(\frac{w_a}{w_f}\right)$ added at station 8.	Equation (A8) of appendix A	$\frac{lb\ air}{lb\ fuel}$	-------	49.29
T_{t_9}	Fig. 3, quadrant IV, for T_{t_6} and $\left(\frac{w_a}{w_f}\right)$ added at station 8.	° R	1584	2926
p_{t_9}/p_0	$\left(\frac{p_{t_3}}{p_0}\right)\left(\frac{p_{t_4}}{p_{t_3}}\right)\left(\frac{p_{t_5}}{p_{t_4}}\right)\left(\frac{p_{t_6}}{p_{t_5}}\right)\left(\frac{p_{t_7}}{p_{t_6}}\right)\left(\frac{p_{t_8}}{p_{t_7}}\right)\left(\frac{p_{t_9}}{p_{t_8}}\right)$	None	11.30	11.30
V_{11}	Fig. 2, quadrants III and IV, and $\left(\frac{p_{t_9}}{p_0}\right)$ and T_{t_9}	$\frac{ft}{sec}$	3118	4297
C_{F_t}'	$2\left[\left(1+\frac{w_f}{w_a}\right)\frac{V_{11}}{V_0}-1\right]$	None	1.256	2.520

° Values for assumed condition of operation.

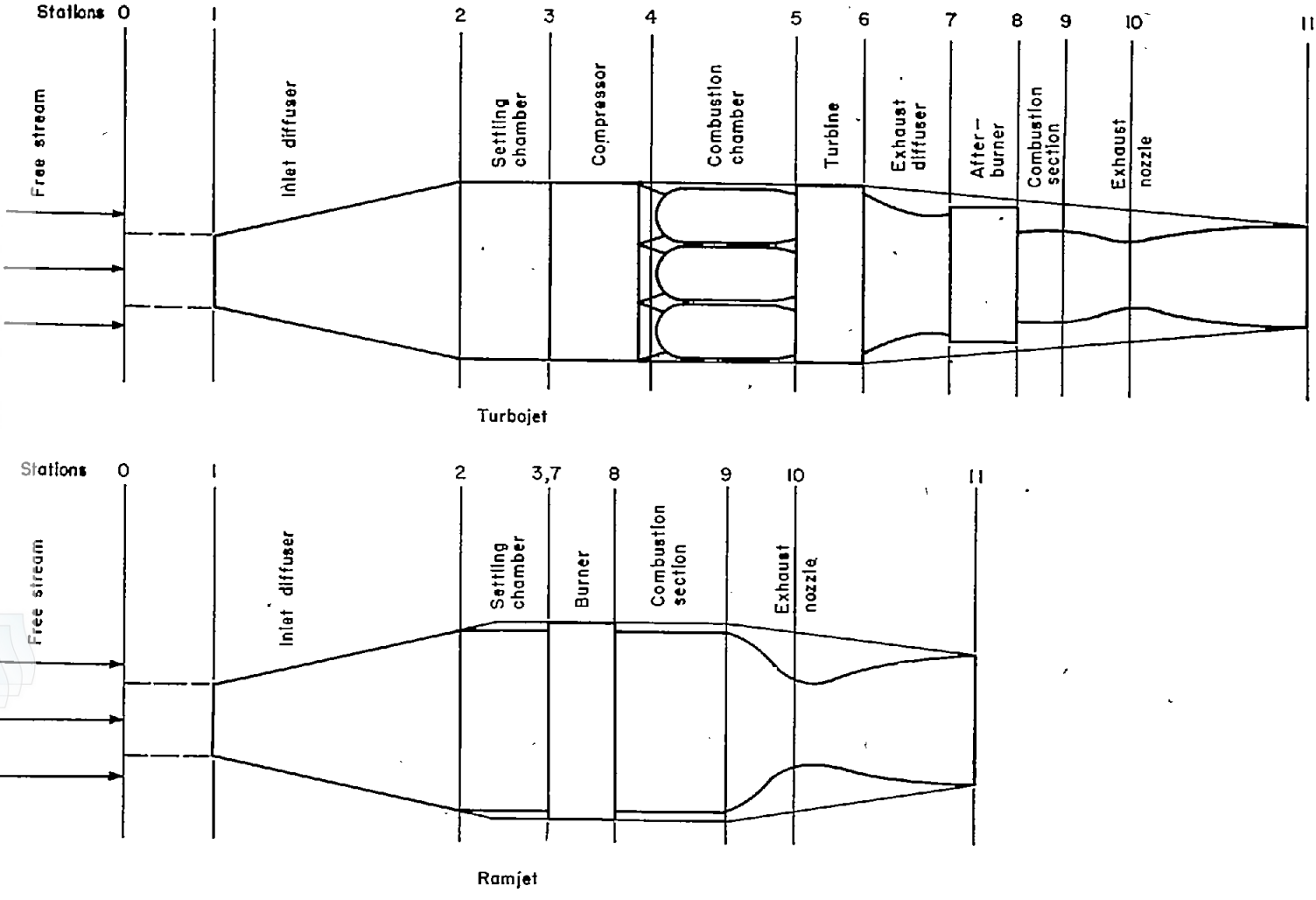

FIGURE 1.—Schematic representation of propulsive systems.

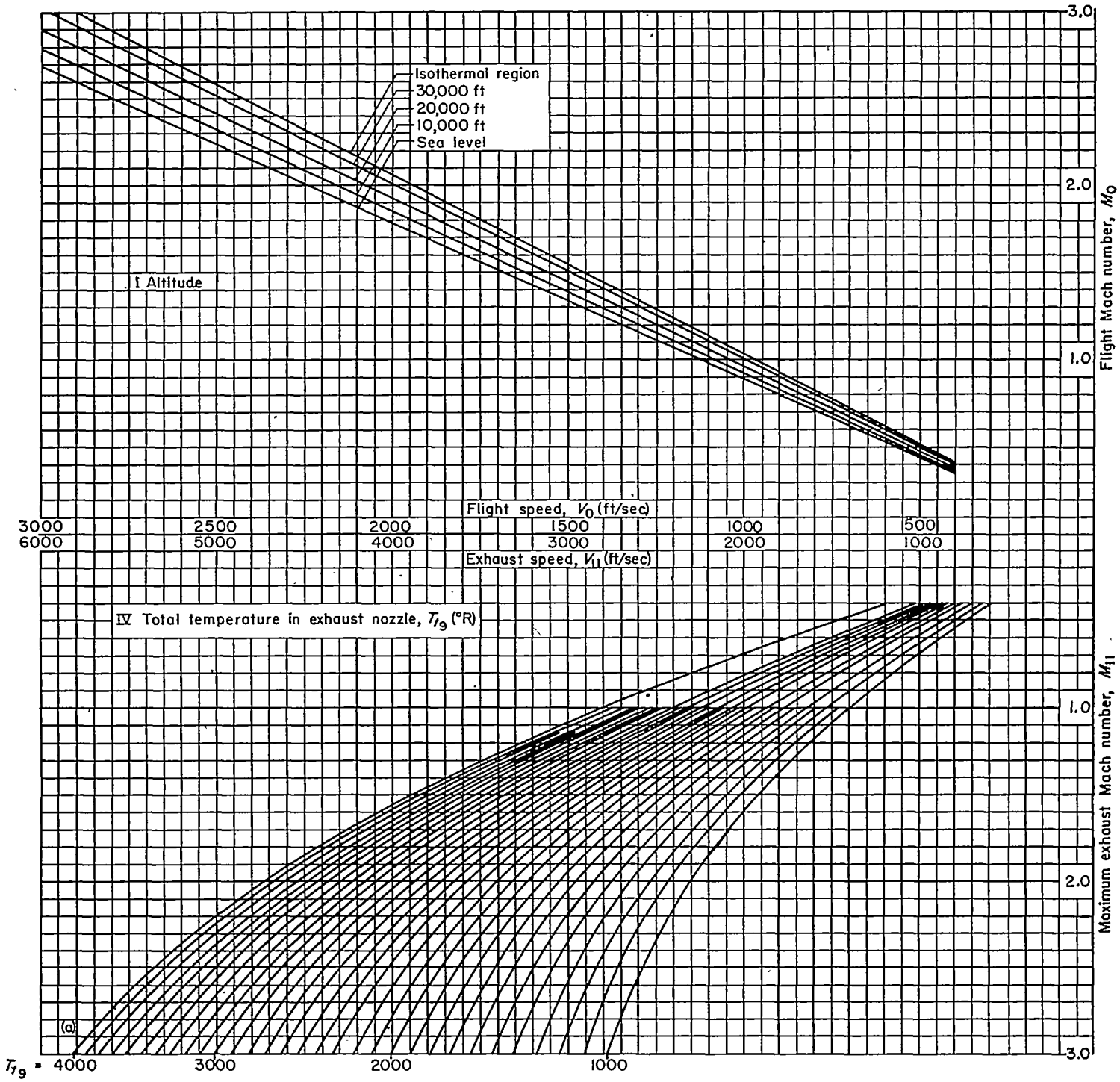

FIGURE 2.—Velocity graph.

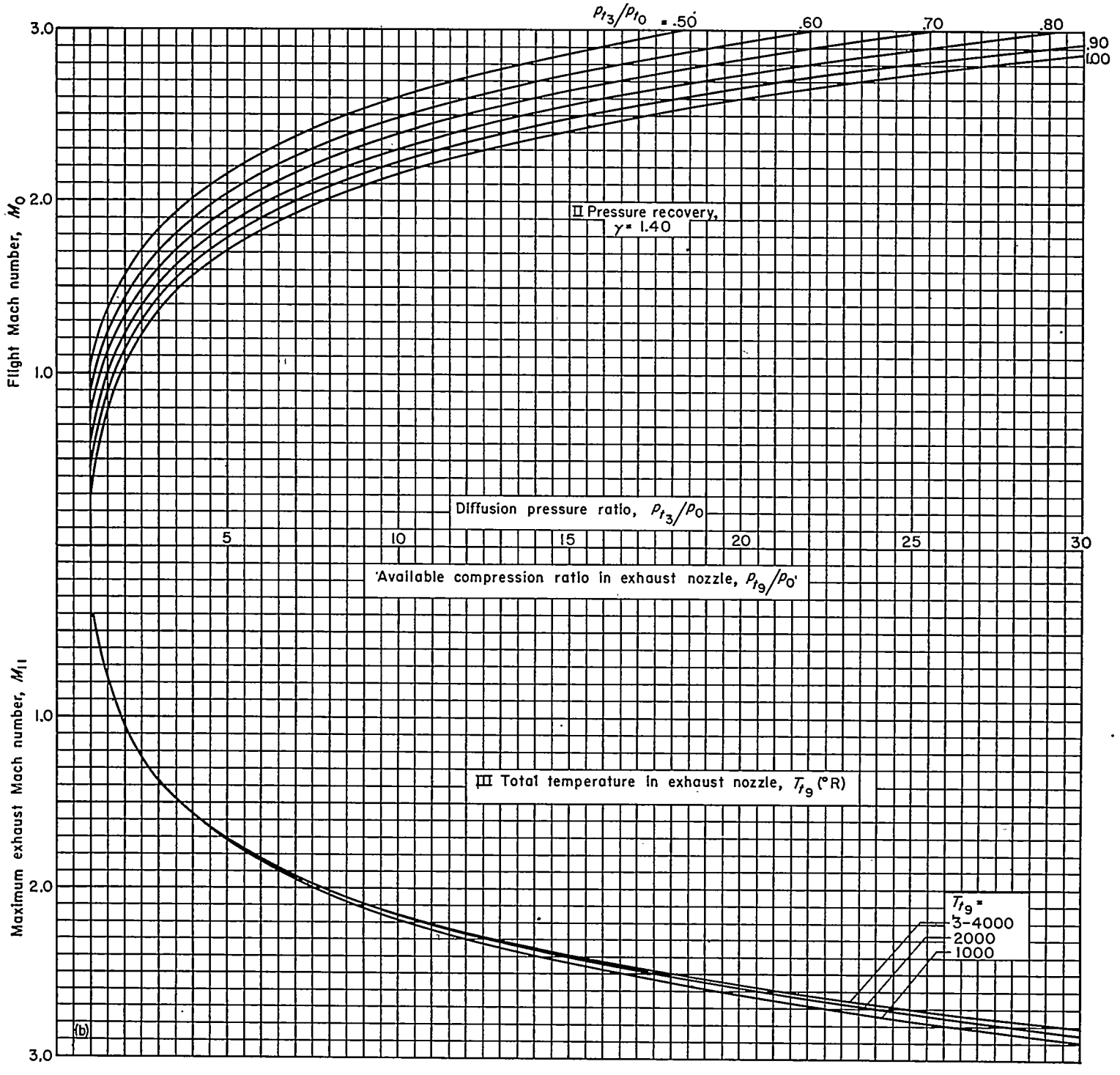

FIGURE 2.—Concluded.

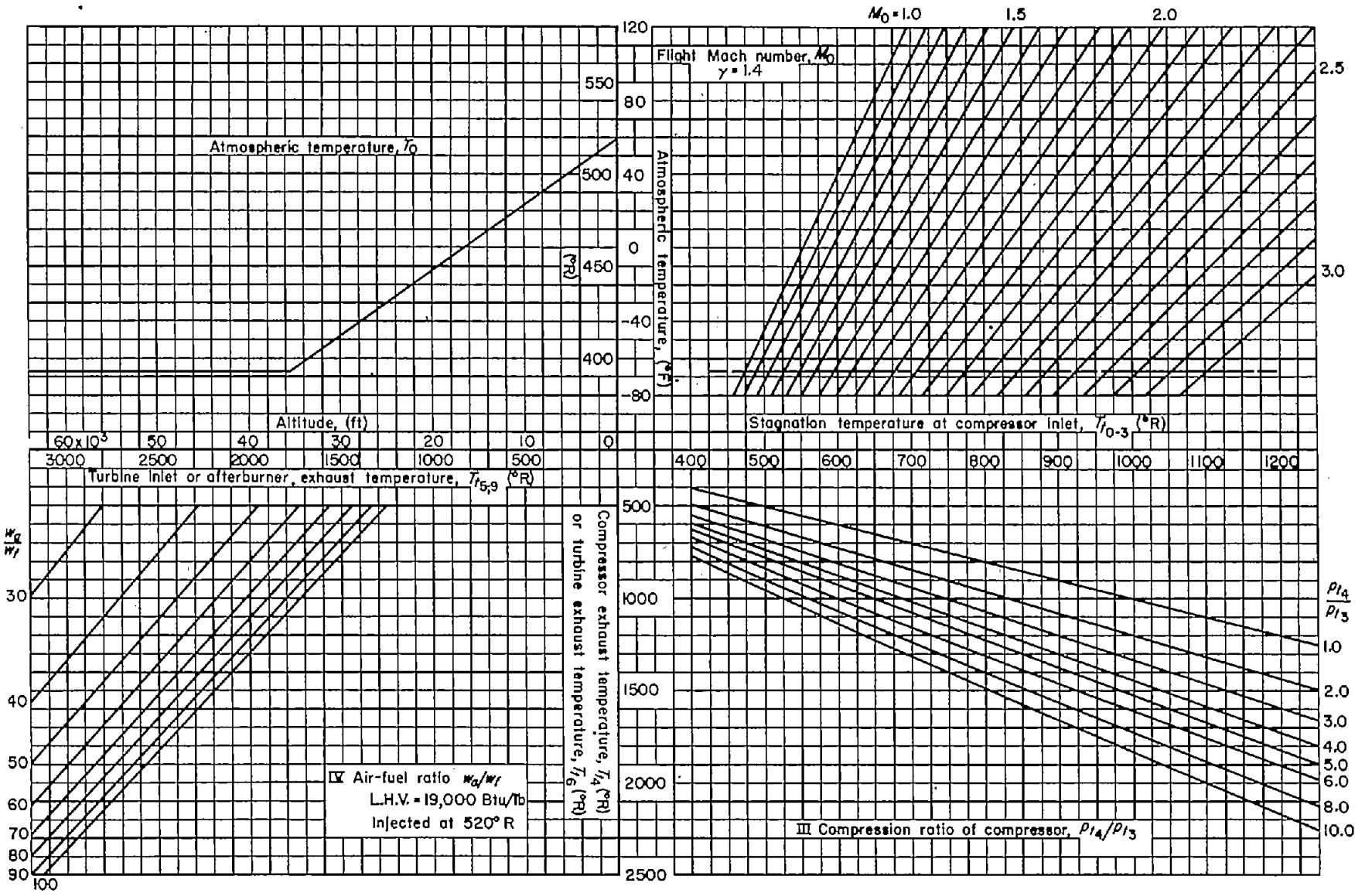

FIGURE 3.—Temperature graph.

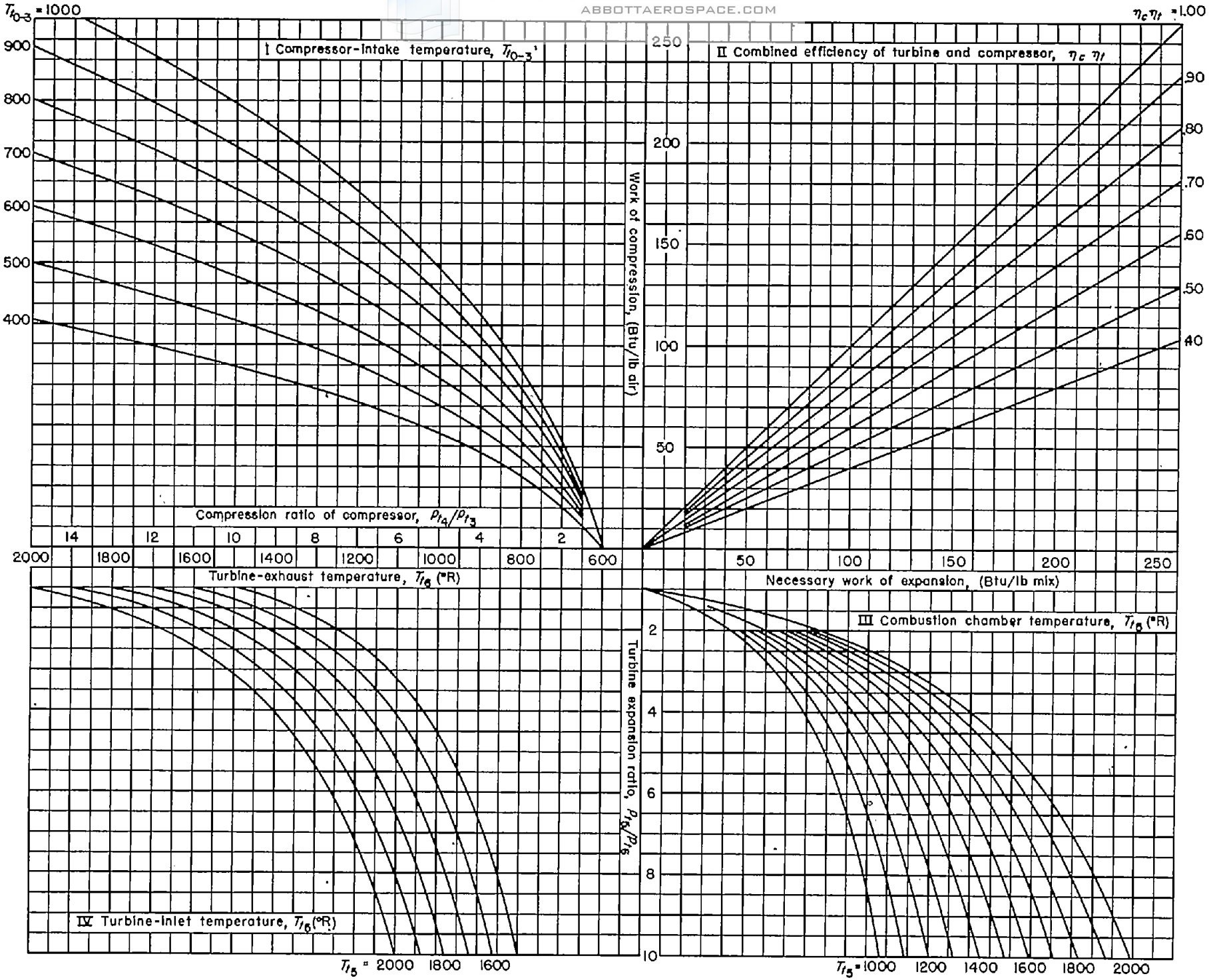

FIGURE 4.—Compressor-turbine graph.

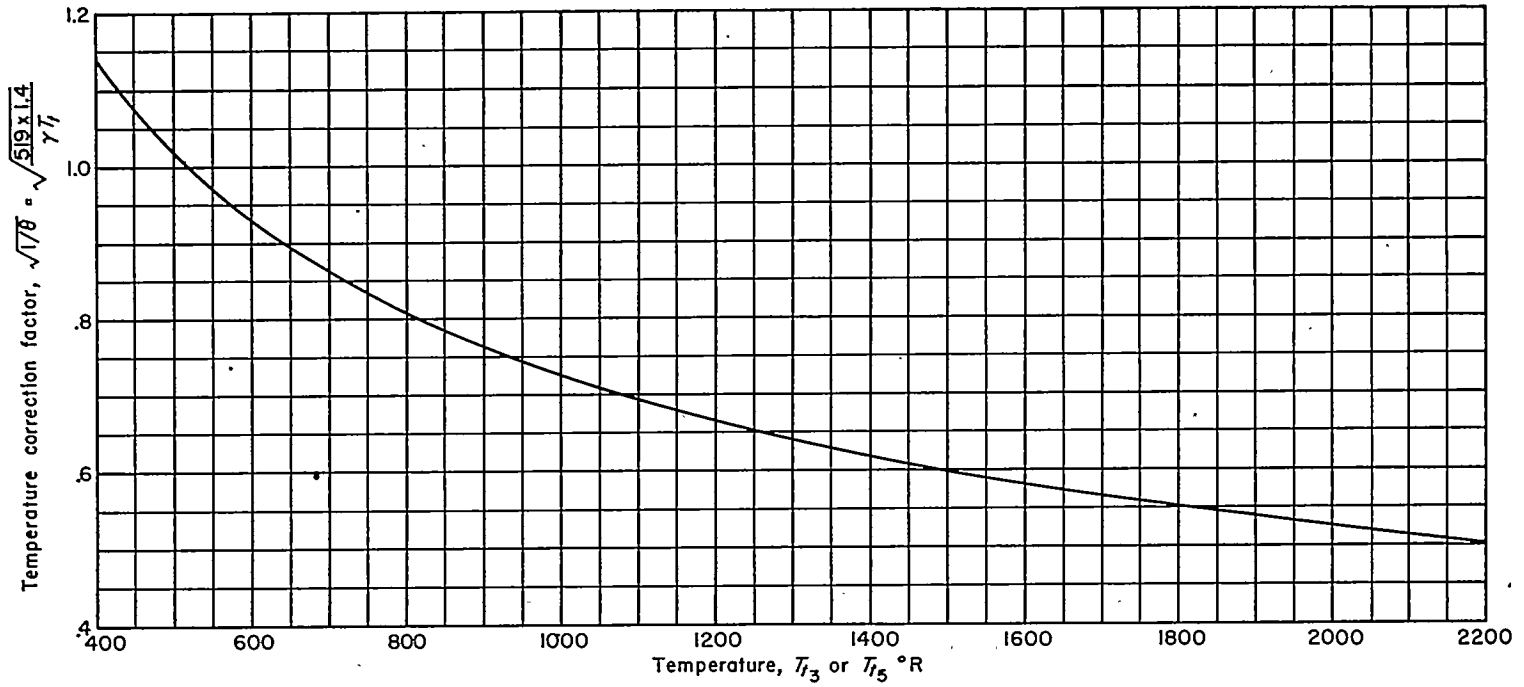

FIGURE 5.—Temperature correction graph.

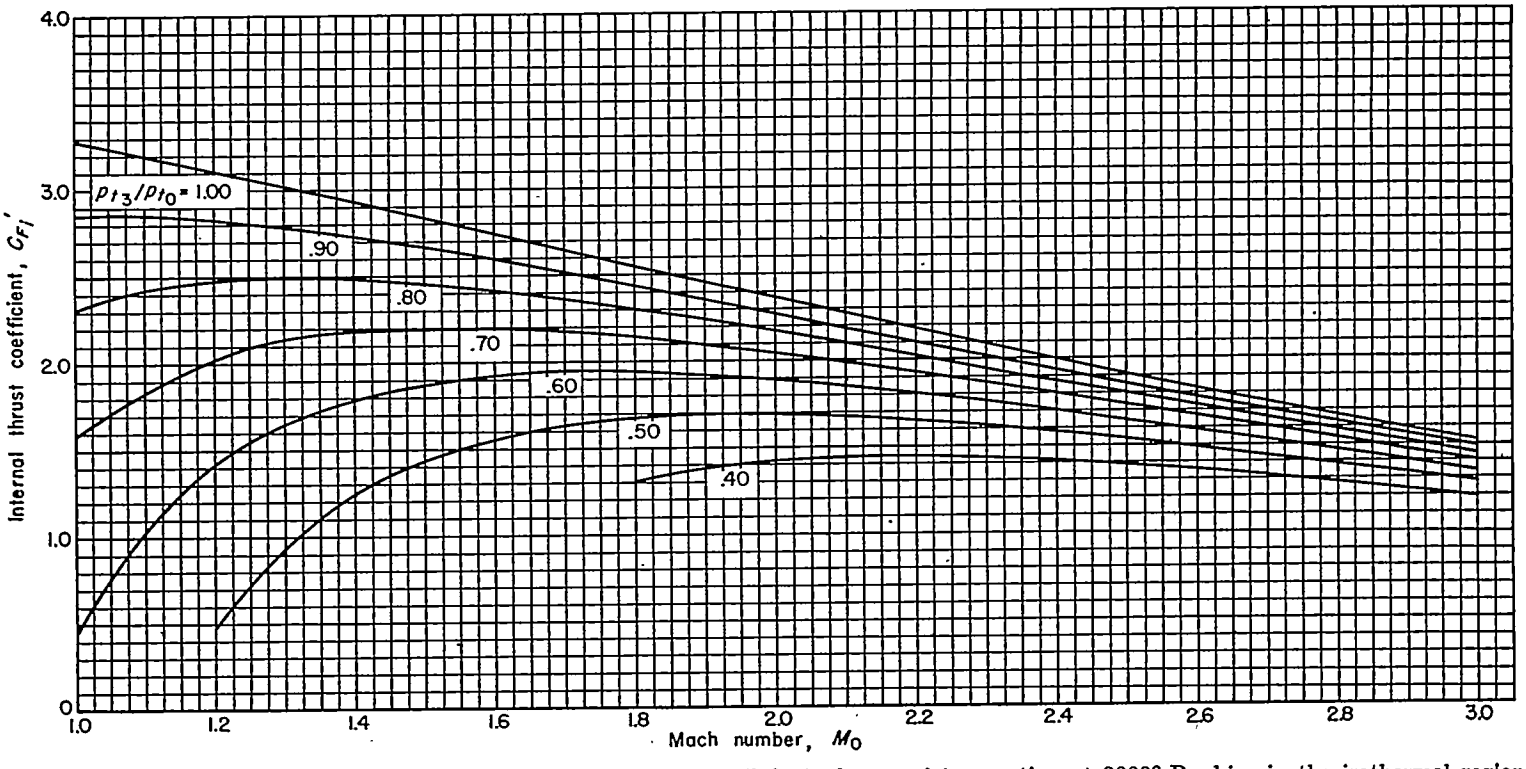

FIGURE 6.—Effects of total-pressure recovery on internal thrust coefficient of a ram jet operating at 3000° Rankine in the isothermal region of atmosphere.

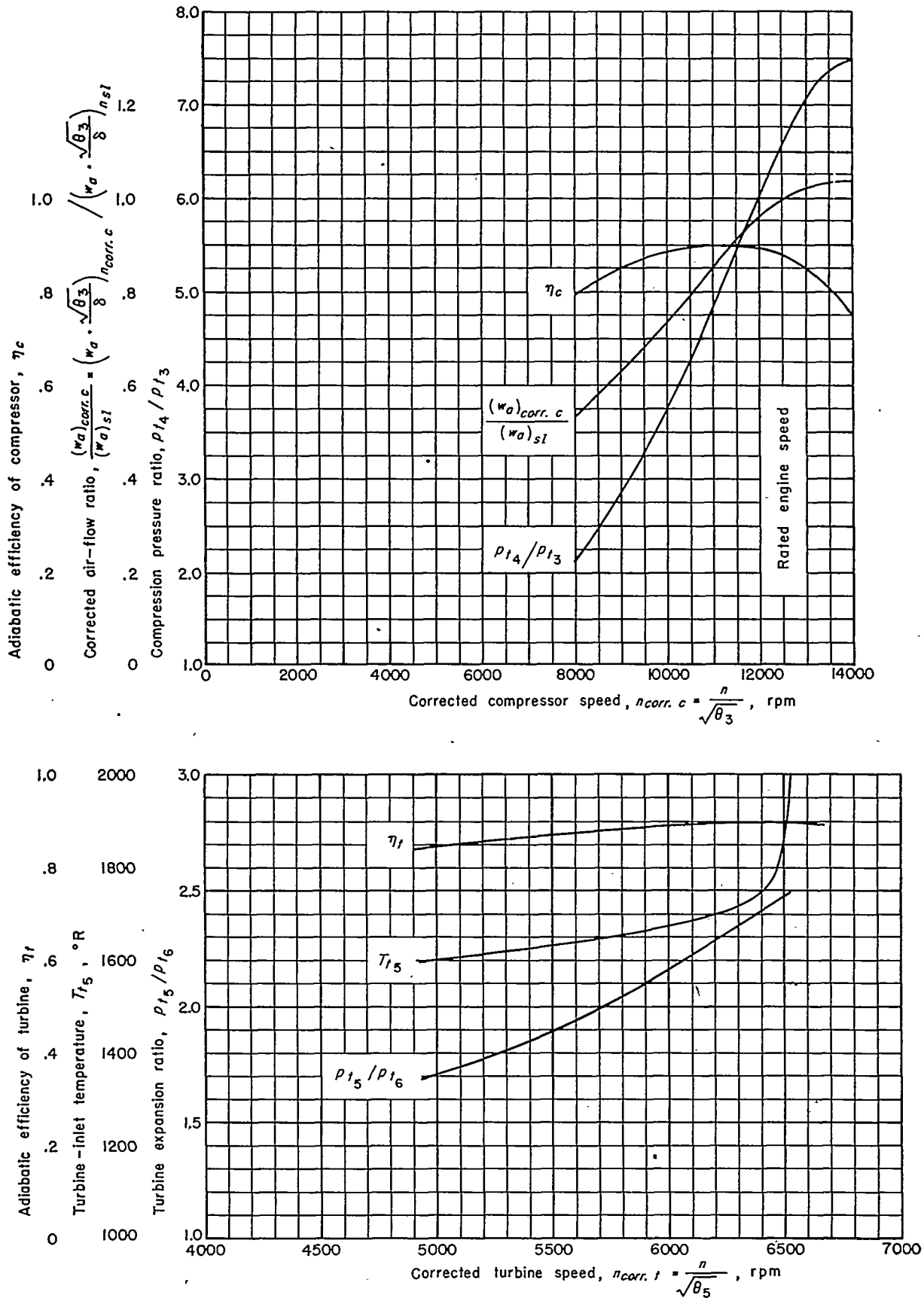

FIGURE 7.—Turbojet-engine characteristics corrected to standard sea-level static atmospheric conditions.

321695—55——51

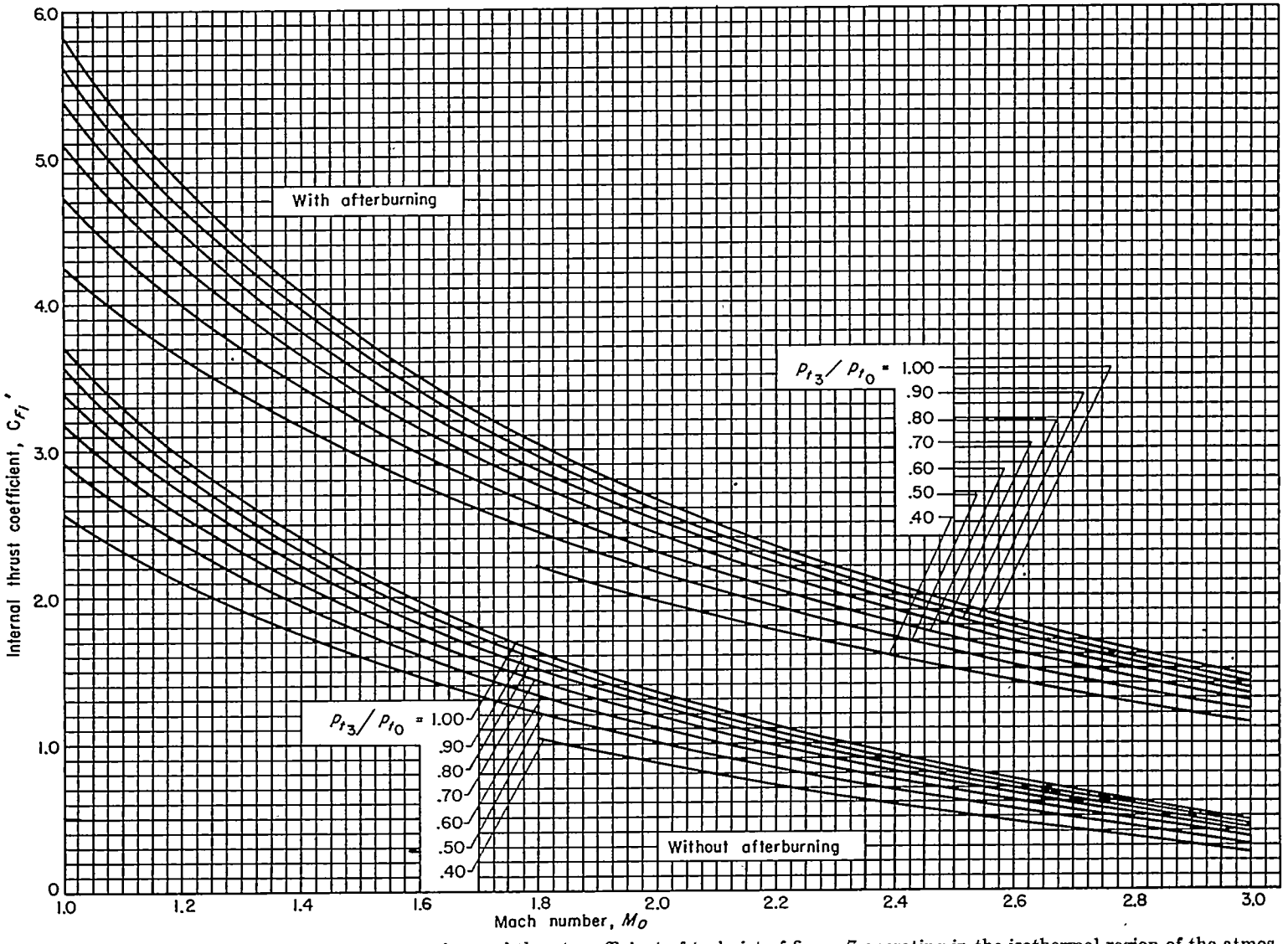

FIGURE 8.—Effects of total-pressure recovery on internal thrust coefficient of turbojet of figure 7 operating in the isothermal region of the atmosphere at 2000° Rankine without afterburning and the same turbojet with afterburning having a total air-to-fuel ratio equal to that of the ram jet of figure 6.

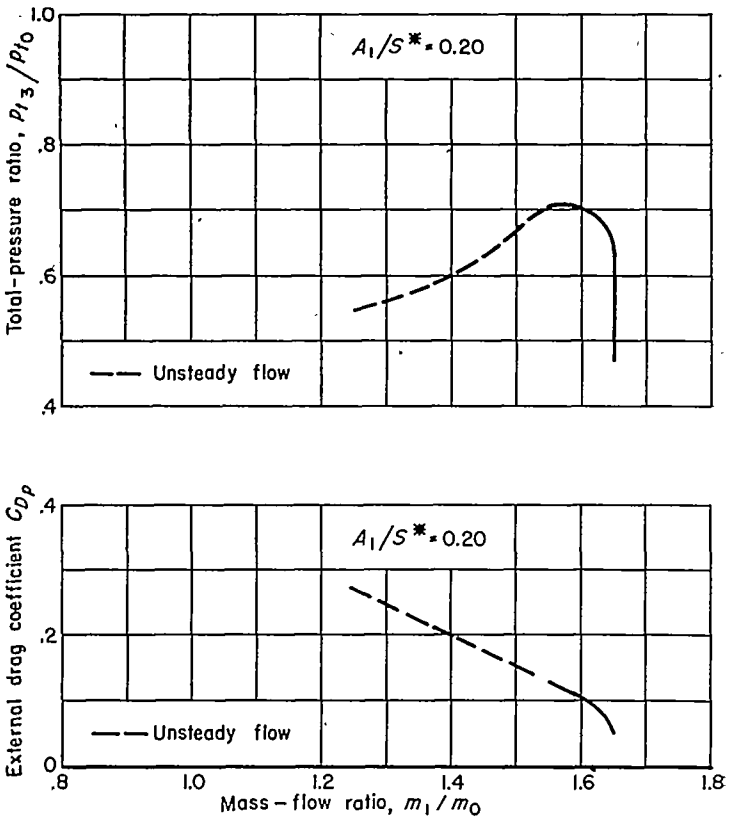

FIGURE 9.—Induction-system characteristics at Mach number 2.5.

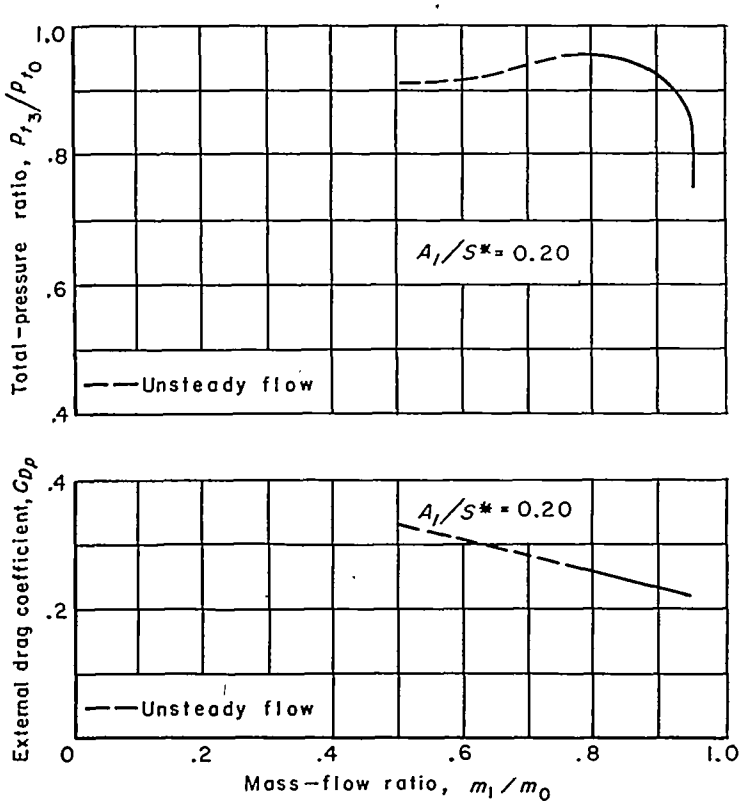

FIGURE 10.—Induction-system characteristics at Mach number 1.2.

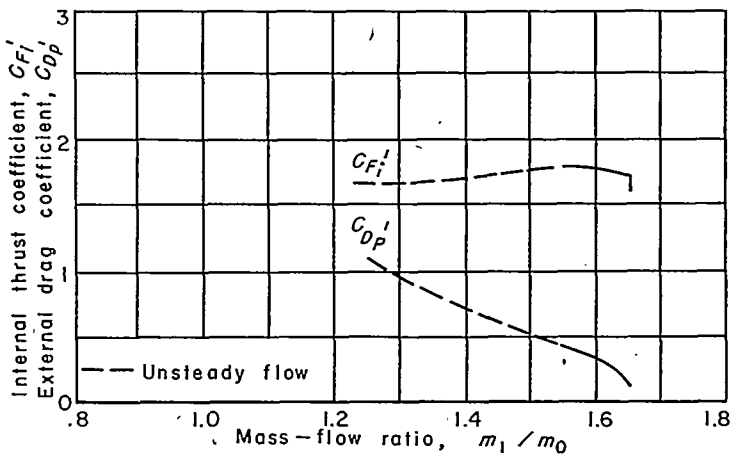

FIGURE 11.—Effects of mass-flow ratio on thrust and drag coefficients.

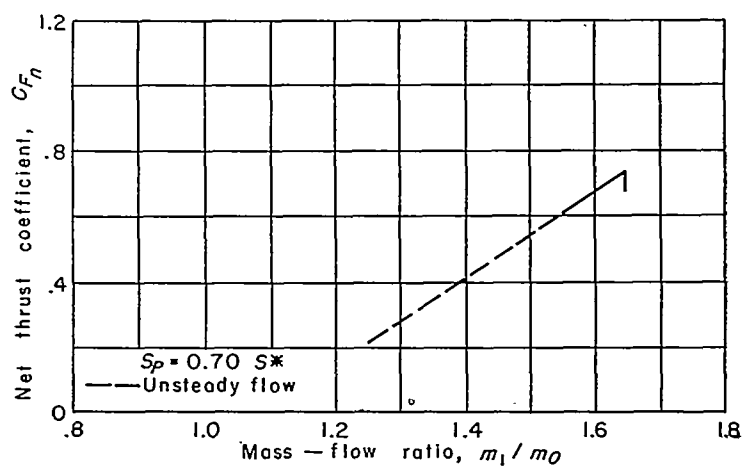

FIGURE 12.—Effects of mass-flow ratio on net thrust coefficient at Mach number 2.5 in the isothermal region of the atmosphere.

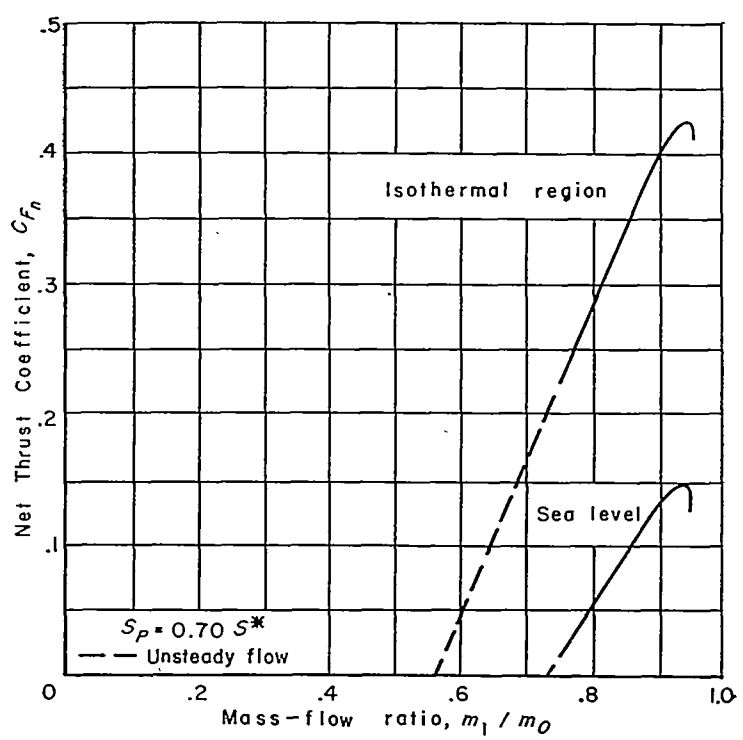

FIGURE 13.—Effects of mass-flow ratio on net thrust coefficient at Mach number 1.2.

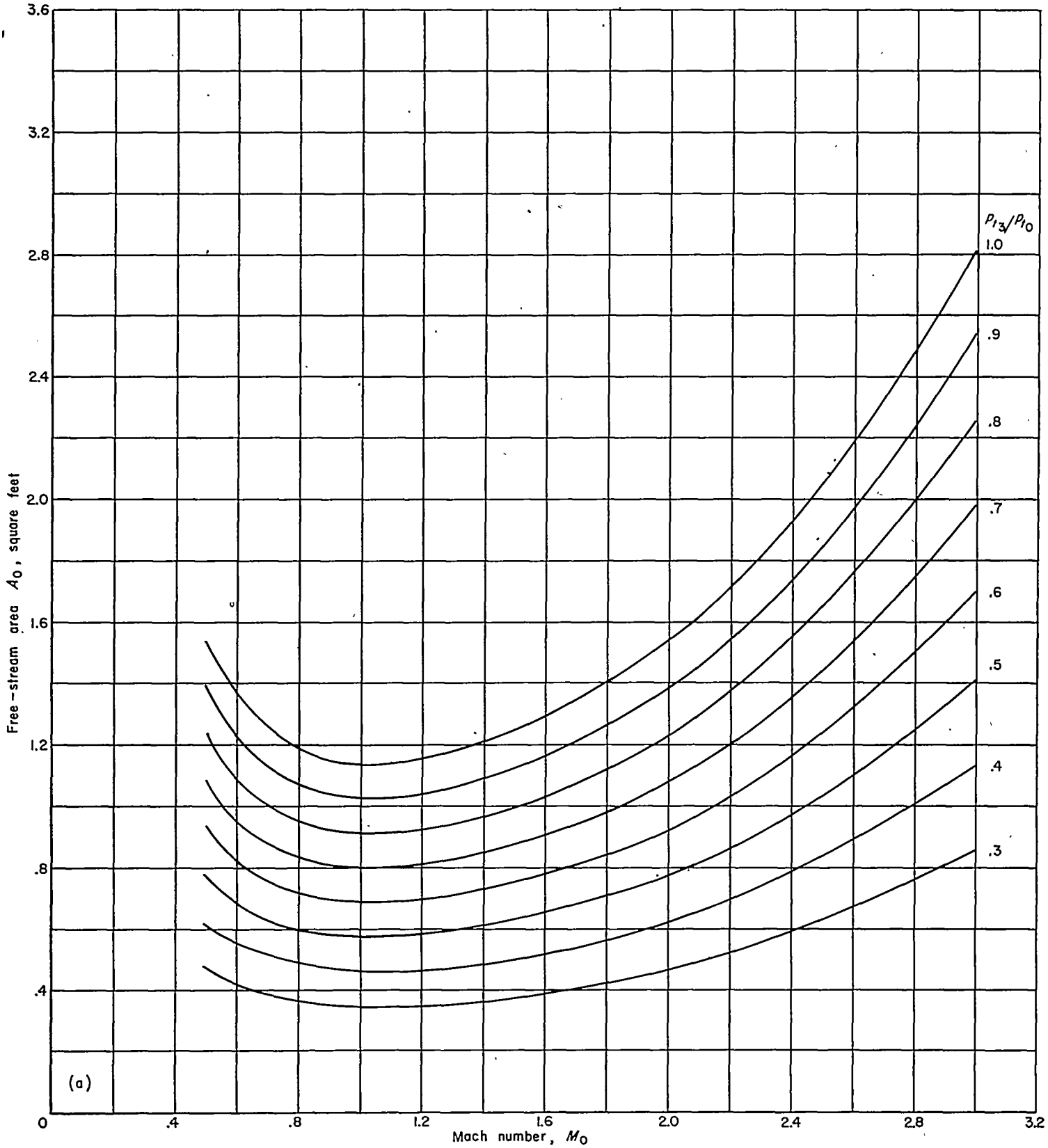

(a) Isothermal region.

FIGURE 14.—Free-stream area required by the turbojet engine of the illustrative examples.

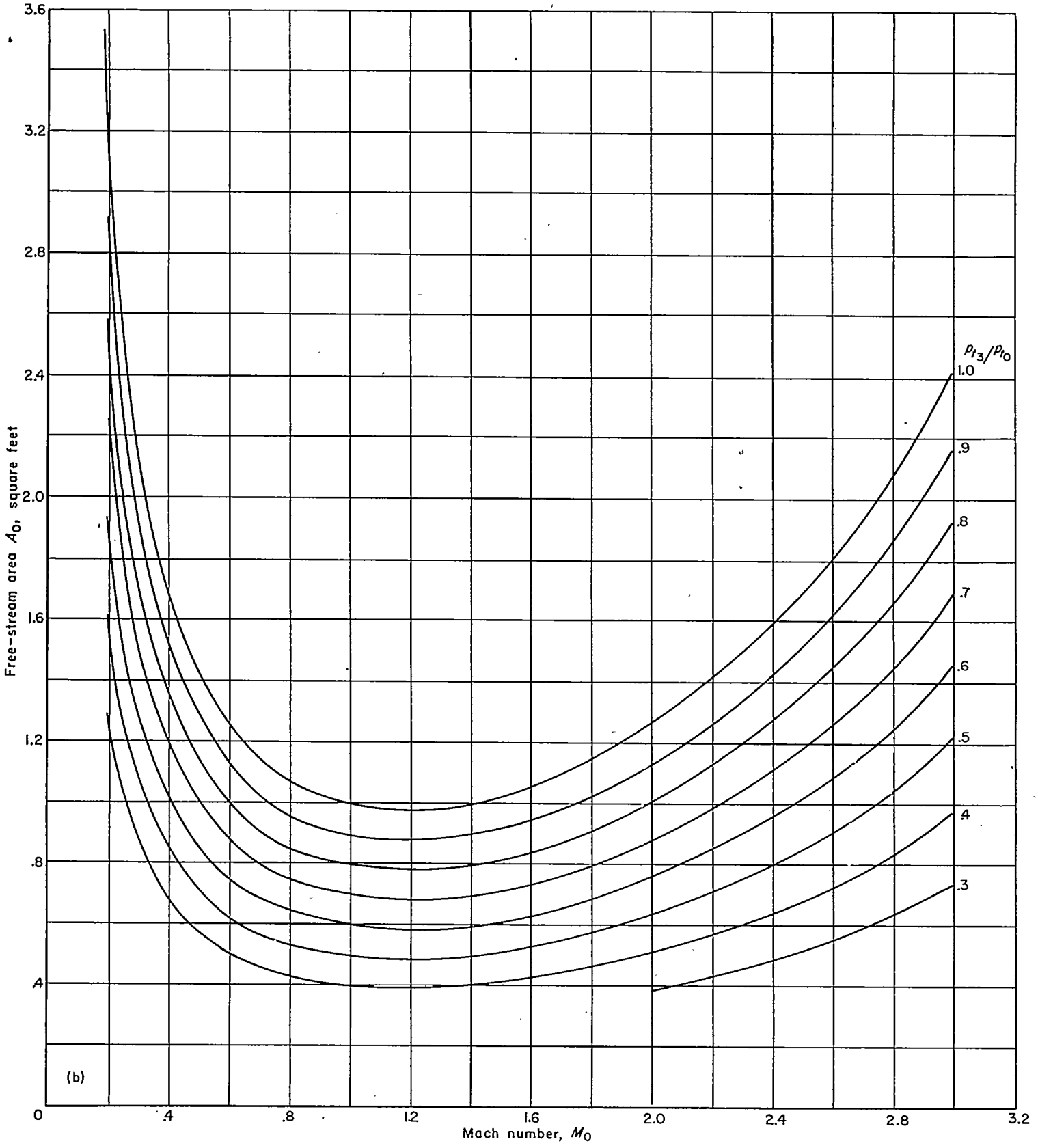

(b) Sea level, standard atmosphere.

FIGURE 14.—Concluded.

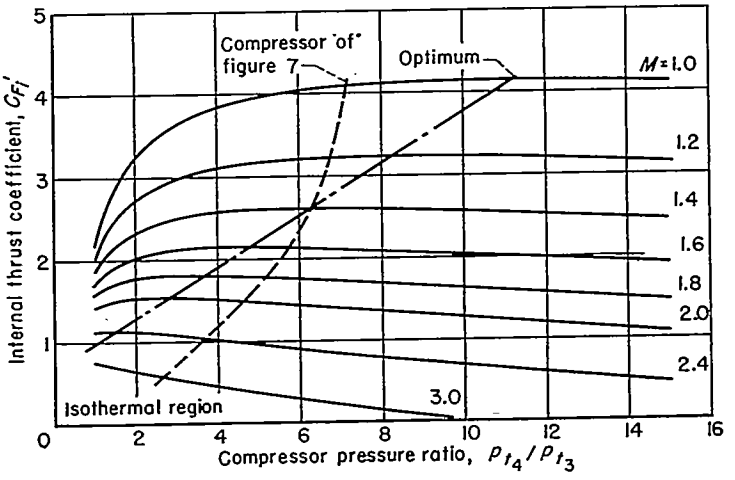

FIGURE 15.—Effects of compressor pressure ratio on internal thrust coefficient of turbojet without afterburning.

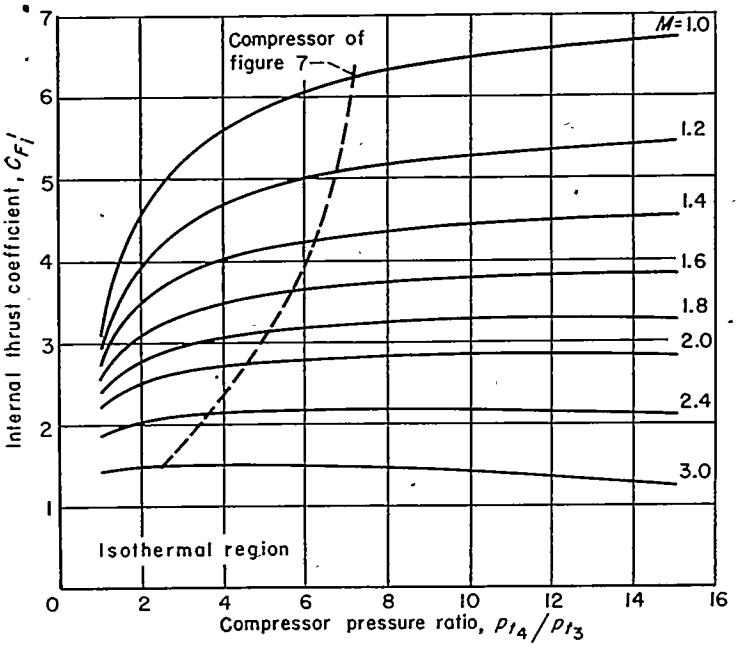

FIGURE 16.—Effects of compressor pressure ratio on internal thrust coefficient of turbojet with afterburning.